Competing Roughening Mechanisms in Strained Heteroepitaxy: A Fast Kinetic Monte Carlo Study

Chi-Hang Lam,[1,2] Chun-Kin Lee,[1] and Leonard M. Sander[2]

[1]*Department of Applied Physics, Hong Kong Polytechnic University, Hung Hom, Hong Kong, China*
[2]*Michigan Center for Theoretical Physics, Department of Physics, Randall Laboratory, University of Michigan, Ann Arbor, Michigan 48109-1120*

(Received 6 July 2002; published 5 November 2002)

We study the morphological evolution of strained heteroepitaxial films using kinetic Monte Carlo simulations in two dimensions. A novel Green's function approach, analogous to boundary integral methods, is used to calculate elastic energies efficiently. We observe island formation at low lattice misfit and high temperature that is consistent with the Asaro-Tiller-Grinfeld instability theory. At high misfit and low temperature, islands or pits form according to the nucleation theory of Tersoff and LeGoues.

DOI: 10.1103/PhysRevLett.89.216102 PACS numbers: 68.65.Hb, 81.16.Dn, 81.16.Rf

Coherent three-dimensional (3D) islands in strained heteroepitaxial films are of great interest because they can self-assemble as quantum dots for possible advanced optoelectronic applications [1,2]. They are observed in a variety of film-substrate combinations including Ge/Si, InAs/GaAs, InAs/InP, etc. In these systems, island formation follows the Stranski-Krastanov mode. Initially, two-dimensional (2D) layer-by-layer growth leads to a flat wetting layer under stress. Beyond a threshold film thickness, 3D islands emerge on top of the wetting layer partially relieving the stress. The precise island formation mechanism is currently under intensive debate. According to the nucleation theory of Tersoff and LeGoues, the growth of stable islands requires overcoming an energy barrier associated with a critical island size [3]. However, experiments reveal gradual development of ripples [4] or prepyramids [5] at the initial stage of island formation. These observations are more consistent with the Asaro-Tiller-Grinfeld (ATG) linear instability theory, which predicts that morphological perturbations at sufficiently long wavelengths grow spontaneously and steadily [6,7]. It was originally proposed for smooth surfaces, but extensions to faceted ones based on nonequilibrium deposition conditions [8] or finite vicinality of substrates [9] have been suggested.

To better understand the roughening mechanism of strained layers, we have performed kinetic Monte Carlo simulations using an atomistic model [10–13]. This approach is computationally very intensive but can reliably account for both lattice discreteness and nonequilibrium conditions. Previous simulations successfully demonstrated island formation in strained layers but only via the nucleation mechanism [10–12]. In this work we introduce significantly more efficient algorithms. Thus we can explore a much wider range of conditions and observe a rich variety of morphologies in better general agreement with experiments. In particular, by lowering the lattice misfit and raising the temperature, the roughening mechanism crosses over from nucleation to instability controlled.

We adopt the 2D ball and spring model of heteroepitaxy defined on a square lattice first studied by Orr *et al.* [10] and subsequently by Barabási [11] and Khor and Das Sarma [12]. Simulations in 3D limited to submonolayer coverage were performed by Meixner *et al.* [13]. Our model parameters are appropriate to the widely studied $Si_{1-x}Ge_x/Si(001)$ system. We assume a substrate lattice constant $a_s = 2.715$ Å so that a_s^3 gives the correct atomic volume in crystalline silicon. The lattice constant a_f of the film material is related to the lattice misfit $\epsilon = (a_f - a_s)/a_f$ which has a compositional dependence $\epsilon = 0.04x$. Nearest and next nearest neighboring atoms are directly connected by elastic springs with force constants $k_N = 13.85\ \mathrm{eV}/a_s^2$ and $k_{NN} = k_N/2$, respectively. This choice gives the correct modulus c_{11} of silicon and a shear modulus constant along tangential and diagonal directions, despite a slight anisotropy in the Young's modulus. The elastic couplings of adatoms with the rest of the system are weak and are completely neglected for better computational efficiency. Solid-on-solid conditions and atomic steps limited to at most two atoms high are assumed. Every topmost atom in the film can hop to a random topmost site s columns away where $s = \pm 1, \pm 2, \ldots,$ or $\pm s_{\max}$ with equal probability. Previous simulations allowed only nearest neighbor hopping (i.e., $s_{\max} = 1$) [10–13]. To speed up the simulations, we put $s_{\max} = 8$ or 20, respectively, for $x > 0.6$ or $x \le 0.6$. These hopping ranges are much shorter than the dimensions of the relevant structures (islands or pits) on the films, and we have checked that decreasing $s_{\max}$ does not alter our results. The hopping rate Γ_m of a topmost atom m follows an Arrhenius form:

$$\Gamma_m = R_0 \exp\left[-\frac{n_m \gamma - \Delta E_m - E_0}{k_B T} \right]. \qquad (1)$$

Here n_m is the number of nearest and next nearest

neighbors of atom m. We choose a bond strength $\gamma = 0.4$ eV which will be explained later. The energy ΔE_m is the difference in the strain energy E_s of the whole lattice at mechanical equilibrium when the site is occupied versus unoccupied. Finally, we put $E_0 = 0.53$ eV and $R_0 = 2D_0/(\sigma_s a_s)^2$ with $D_0 = 3.83 \times 10^{13}$ Å^2 s^{-1} and $\sigma_s^2 = \frac{1}{6}(s_{\max} + 1)(2s_{\max} + 1)$. This gives the appropriate adatom diffusion coefficient for silicon (100) [14]. Our model follows detailed balance.

The simulations involve intensive computations resulting solely from the long-range nature of elastic interactions. Practically all the CPU time is spent on the repeated calculations of E_s which is needed to find ΔE_m and hence Γ_m in Eq. (1). The elastic problem is formulated as follows. First, a flat film is homogeneously strained [2]. This provides a convenient reference position with displacement $\vec{u}_i = 0$ for every atom i. In general, the elastic force on atom i by a directly connected neighbor j is $\vec{f}_{ij} = -\mathbf{K}_{ij}(\vec{u}_i - \vec{u}_j) + \vec{b}_{ij}$ after linearization where the 2×2 symmetric matrix $\mathbf{K}_{ij} = k_{ij}\hat{n}_{ij}\hat{n}_{ij}^t$ is the modulus tensor and $\vec{b}_{ij} = (l_{ij}^0 - l_{ij})\mathbf{K}_{ij}\hat{n}_{ij}$ arises from the homogeneous stress in flat films. The spring constant k_{ij} equals either k_N or k_{NN} for tangential or diagonal connection, respectively. The unit column vector $\hat{n}_{ij}$ points from the unstrained lattice position of atom j towards that of atom i, and t denotes transpose. Furthermore, l_{ij}^0 and l_{ij} are, respectively, the natural and homogeneously strained spring lengths which follow easily from a_s and ϵ. Mechanical equilibrium requires $\sum_j \vec{f}_{ij} = 0$ for each atom i. This leads to a large set of equations coupling the $\vec{u}_i$ of *all* of the atoms. The solution then gives the elastic energy stored in every spring and hence E_s.

We now introduce a Green's function approach for calculating E_s efficiently requiring the explicit consideration of *only* the surface atoms. It is a lattice analogue of boundary integral methods and is superior to boundary element techniques for our intrinsically discrete problem. We first derive the exact formalism. Figure 1 shows an example of a small lattice of atoms (solid circles). As a mathematical construct, we extend the lattice by adding *ghost* atoms (open circles) with similar elastic properties. Unphysical couplings are hence introduced but can be exactly canceled by applying *external* forces $\vec{f}_j^{\,e}$ and $\vec{f}_{j'}^{\,e}$ to every real surface atom j and ghost surface atom j', respectively, with

$$\vec{f}_j^{\,e} = \sum_{j'} (\mathbf{K}_{jj'}\vec{u}_j - \vec{b}_{jj'}), \tag{2}$$

$$\vec{f}_{j'}^{\,e} = -\sum_j \mathbf{K}_{jj'}\vec{u}_j. \tag{3}$$

The summation in Eq. (2) is over each ghost atom j' connected directly to the real atom j, and it is analogous in Eq. (3). It is easy to see that the real atoms are then exactly decoupled from the ghost atoms which are held precisely at their homogeneously strained positions.

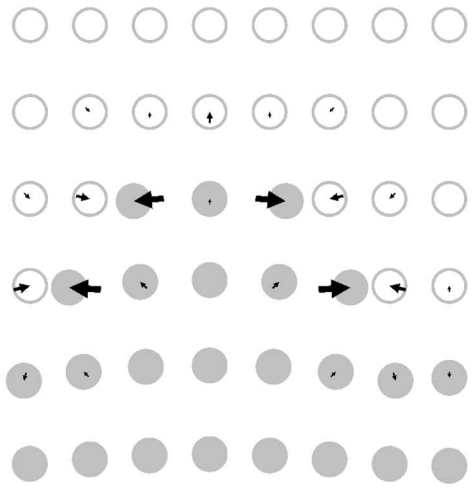

FIG. 1. Ghost atoms (open circles) are added on top of the real atoms (solid circles) forming an extended lattice. Unphysical couplings are exactly canceled by external forces (arrows) applied to the real and ghost surface atoms.

A lattice Green's function is then applied to express the displacement, $\vec{u}_i$, of every real surface atom i under the influence of the external forces:

$$\vec{u}_i = \sum_j \mathbf{G}_{ij}\vec{f}_j^{\,e} + \sum_{j'} \mathbf{G}_{ij'}\vec{f}_{j'}^{\,e}. \tag{4}$$

Note that the Green's function $\mathbf{G}$ is defined for the extended lattice and is *independent of the film morphology*. It can thus be computed numerically once prior to the start of the simulation. It should not be confused with the half-plane Green's function which provides simpler but only approximate results [3,13]. Combining Eqs. (2)–(4), we arrive at the reduced set of equations

$$\vec{u}_i = \sum_{jj'} [(\mathbf{G}_{ij} - \mathbf{G}_{ij'})\mathbf{K}_{jj'}\vec{u}_j - \mathbf{G}_{ij}\vec{b}_{jj'}] \tag{5}$$

coupling only the real surface atoms where the sum is over all pairs of directly connected real and ghost surface atoms j and j', respectively. The solution of Eq. (5) gives $\vec{u}_i$.

The elastic energy E_s can then be calculated directly from

$$E_s = E_s^0 - \frac{1}{2}\sum_{jj'} \vec{b}_{jj'} \cdot \vec{u}_j, \tag{6}$$

which is derived from a simple consideration of virtual work. Here the sum is defined similarly to that in Eq. (5), and E_s^0 equals the unrelaxed value of E_s when $\vec{u}_i \equiv 0$ which can be straightforwardly computed. The method summarized in Eqs. (5) and (6) is exact and practical for simulations at moderate scales.

We can go further and use a coarse-grained version of our Green's function approach for a further boost on the computational efficiency. Finding the strain energy ΔE_m

of the atom m needed in Eq. (1) requires calculating the strain energy E_s of the whole lattice twice with and without the atom m. Certain fine details of the surface far away are obviously unimportant and can be neglected. Specifically, surface atoms are grouped into sets with the Ith of them denoted by Ω_I. We neglect fluctuations within a set by assuming identical displacement $\vec{u}_i \equiv \vec{u}_I$ for each member $i \in \Omega_I$. Equation (5) is then approximated as

$$\vec{u}_I = \sum_J \left[\sum_{j \in \Omega_J, j'} (\mathbf{G}_{Ij} - \mathbf{G}_{Ij'}) \mathbf{K}_{jj'} \right] \vec{u}_J - \sum_{jj'} \mathbf{G}_{Ij} \vec{b}_{jj'}, \quad (7)$$

where $\mathbf{G}_{Ij} = \mathbf{G}_{ij}$ with the lattice point i at the centroid of the set Ω_I. Every atom within three columns from the atom m is not coarsened and constitutes its own single-membered set. Farther away at r columns from the atom m, sets contain atoms in neighborhoods of $2r/3 + 1$ columns wide, a form motivated by simple error analysis. We have checked numerically that a smaller degree of coarsening leads to no noticeable difference in our results.

Surface diffusion can be simulated using the hopping rates in Eq. (1) as ΔE_m is now readily computable. We adopt an acceptance-rejection algorithm aided by tabulated values of ΔE_m for 5^8 sample surface configurations. Details will be explained elsewhere. In our main simulations, the lattice is of 1024 atoms wide following periodic boundary conditions. The substrate is 1024 monolayers (ML) thick while the extended lattice on which we compute the Green's function includes also a film of 80 ML. Fixed boundary conditions are applied to the top and bottom layers of the extended lattice.

We first simulate deposition of pure Ge film (i.e., $x = 1$) with misfit $\epsilon = 4\%$ at temperature $T = 600$ K. At very high deposition rate $R = 80$ ML s^{-1} [Fig. 2(a)], we observe layer-by-layer growth. At slower deposition rate $R = 8$ ML s^{-1} [Fig. 2(b)], the film is initially flat but pits then develop. A detailed examination of the morphological evolution indicates that the pits appear rather independently and suddenly. Once created, they are immediately bounded by sidewalls at an energetically favorable 45° inclination. These features strongly support the nucleation mechanism for their formation, noting that pits are energetically more favorable than islands [3]. This pit nucleation process is similar to that in Fig. 1(d) of Ref. [10]. At $R = 0.8$ ML s^{-1} [Fig. 2(c)], islands with 45° sidewalls nucleate at a very early stage before the film is sufficiently thick for pit formation. The result is analogous to those in Fig. 1(a) of Ref. [10] and also Refs. [11,12]. Further decreasing R towards realistic values of order $R = 0.01$ ML s^{-1} leads to similar but more widely separated islands.

Figure 3 shows results for deposition at misfit $\epsilon = 2\%$ with $x = 0.5$ at $T = 1000$ K. Depending on R, we observe analogous layer-by-layer growth [Fig. 3(a)], layer-by-layer growth followed by roughening [Fig. 3(b)], and island growth [Fig. 3(c)]. However, the islands in Figs. 3(b) and 3(c) emerge gradually from ripplelike perturbations with local surface inclinations increasing steadily and relatively synchronously in agreement with experiments [4,15,16] and ATG instability theory [6,7]. This regime has not been reported in previous atomistic simulations mainly due to inaccuracies in accounting for the long-range parts of the elastic interactions or the rather thin substrates used [10–13]. Instead, it was observed in continuum simulations [17], which, however, cannot realize the nucleation mechanism.

The importance of the lattice misfit in deciding the roughening mechanism is particularly easy to understand. The nucleation of islands or pits occurs at a rate $R_{\text{nucl}} \sim \exp(-c\epsilon^{-4})$ with c being a constant [3] and becomes very slow at small ϵ [16]. The ATG instability with a roughening rate $R_{\text{inst}} \sim \epsilon^8$ [7] then dominates. For Figs. 2(b) and 3(b), we have chosen deposition rates close to the relevant roughening rates. We then observe kinetically limited wetting layers prior to roughening which is characteristic of Stranski-Krastanov growth. However, the threshold thickness depends strongly on R contrary to experimental findings [2]. A more realistic model in the future should include other mechanisms such as film-substrate interactions [18] or nonlinear elasticity [9] which have been argued to give a more stable wetting layer.

We have also simulated annealing of initially flat films of 30 ML at $T = 1000$ K. At this high temperature, roughening is mainly due to the ATG instability, and we observe the development of ripples followed by islands. Figure 4 shows the surface profiles after the islands are fully developed. The cusps on the surfaces [19] are

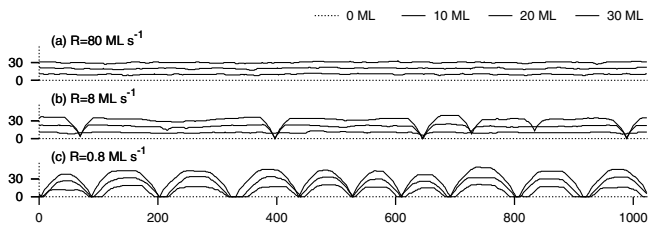

FIG. 2. Simulations of deposition of Ge films at $T = 600$ K with substrate width and thickness both equal $1024a_s \simeq 2780$ Å. The axes are in unit of a_s.

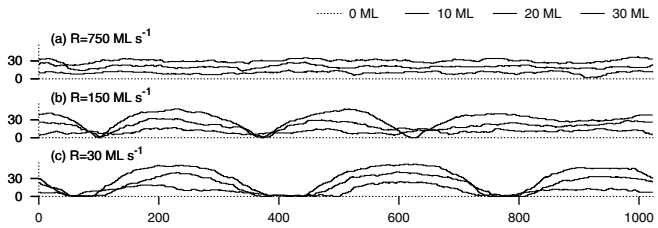

FIG. 3. Simulations of deposition of $Si_{0.5}Ge_{0.5}$ films at $T = 1000$ K.

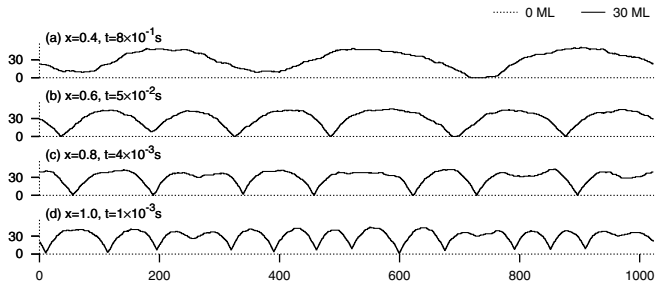

FIG. 4. Simulations of annealing of initially flat $Si_{1-x}Ge_x$ films of 30 ML at $T = 1000$ K for a period of time t.

limited by either the substrate or the local step height limit imposed in our model. We have measured the island size l from power spectra of 11 realizations of similar surfaces. We obtain $l \sim x^{-1.8}$ in reasonable agreement with x^{-2} from the instability theory [6] but slightly different from x^{-1} from experiments [15,16]. The discrepancy with experiments may be improved if the compositional dependence of film properties such as bond energies and diffusion coefficients are properly considered. The island sizes in general lie within the experimental range due to our choice of the bond strength $\gamma = 0.4$ eV, which, in fact, is a reasonable value.

We have already discussed possible extensions of the model to include film-substrate chemical interactions, nonlinear elasticity, and composition-dependent material properties. In our 2D model, starting from (01) surfaces, (11) facets at an inclination of 45° can be obtained. Other facets are energetically unstable and are not observed. To enhance the morphological resemblance with experiments in which (105) and (113) facets are found [4], one can explore more sophisticated forms of bond energies favoring appropriate 2D analogs of them.

The ATG theory assumes a nonsingular form of the equilibrium surface energy which applies to all 2D surfaces at finite temperatures. In 3D, the surface energy is instead singular in the presence of facets at the relevant temperatures below the roughening transition. Therefore, the validity of the ATG instability is not clear [2,8,9]. Critical tests of the theory by 3D simulations are important, and may be feasible using our method. For example, our 2D simulation leading to Fig. 2(b) involves about 6×10^7 hops and ran for 18 h on a pentium 2 GHz computer. Thus, extensions to 3D should be practical.

In conclusion, using accelerated algorithms which properly and efficiently account for long-range elastic interactions, we have simulated deposition and annealing of strained heteroepitaxial layers in 2D. At low misfit and high temperature, we observe ripples and subsequently gradual island formation consistent with the ATG instability theory. At high misfit and low temperature, islands or pits are generated via the nucleation pathway. These suggest a nontrivial competition between roughening mechanisms, although reliable quantitative determination of the crossover conditions is beyond the scope of our model. The ATG instability is the most promising description of island formation in $Si_{1-x}Ge_x$ films at low, and probably also at high lattice misfit [4,5]. However, the nucleation mechanism applied to high misfit regimes in certain experimental situations has not been ruled out [20]. Thus the competition of mechanisms can be important for interpreting experimental results. In our simulations, for deposition rates close to the relevant roughening rate, kinetically limited wetting layers develop prior to roughening. At lower but more realistic deposition rates, islands form at an early stage and are more widely separated. This may be related to the great variation in how closely the islands are packed under various conditions in experiments [4,5].

We thank B. G. Orr for helpful comments. This work was supported by HK RGC, Grant No. PolyU-5289/02P and HK PolyU, Grant No. 5309/01P.

[1] V. A. Shchukin and D. Bimberg, Rev. Mod. Phys. **71**, 1125 (1999).
[2] P. Politi, G. Grenet, A. Marty, A. Ponchet, and J. Villain, Phys. Rep. **324**, 271 (2000).
[3] J. Tersoff and F. K. LeGoues, Phys. Rev. Lett. **72**, 3570 (1994).
[4] J. A. Floro *et al.*, Phys. Rev. B **59**, 1990 (1999).
[5] A. Vailionis *et al.*, Phys. Rev. Lett. **85**, 3672 (2000).
[6] R. J. Asaro and W. A. Tiller, Metall. Trans. **3**, 1789 (1972); M. A. Grinfeld, J. Nonlinear Sci. **3**, 35 (1993).
[7] D. J. Srolovitz, Acta Metall. **37**, 621 (1989); B. J. Spencer, P. W. Voorhees, and S. H. Davis, J. Appl. Phys. **73**, 4955 (1993).
[8] J. Tersoff, Phys. Rev. Lett. **87**, 156101 (2001).
[9] H. R. Eisenberg and D. Kandel, cond-mat/0201238.
[10] B. G. Orr, D. A. Kessler, C. W. Snyder, and L. M. Sander, Europhys. Lett. **19**, 33 (1992).
[11] A.-L. Barabási, Appl. Phys. Lett. **70**, 2565 (1997).
[12] K. E. Khor and S. Das Sarma, Phys. Rev. B **62**, 16 657 (2000).
[13] M. Meixner *et al.*, Phys. Rev. Lett. **87**, 236101 (2001).
[14] D. E. Savage *et al.*, in *Semiconductors and Semimetals*, edited by R. Hull and J. C. Bean (Academic Press, New York, 1999), Vol. 56.
[15] R. M. Tromp, F. M. Ross, and M. C. Reuter, Phys. Rev. Lett. **84**, 4641 (2000).
[16] P. Sutter and M. G. Lagally, Phys. Rev. Lett. **84**, 4637 (2000).
[17] W. H. Yang and D. J. Srolovitz, Phys. Rev. Lett. **71**, 1593 (1993); J. Müller and M. Grant, Phys. Rev. Lett. **82**, 1736 (1999).
[18] J. Tersoff, Phys. Rev. B **43**, 9377 (1991).
[19] H. Gao and N. D. William, Annu. Rev. Mater. Sci. **29**, 173 (1999).
[20] M. Kästner and B. Voigtländer, Phys. Rev. Lett. **82**, 2745 (1999).